Scientific African 8 (2020) e00452

Contents lists available at ScienceDirect

Scientific African

journal homepage: www.elsevier.com/locate/sciaf

Effect of calcination temperature on hydroxyapatite developed from waste poultry eggshell

O.G. Agbabiaka[a], I.O. Oladele[a,*], A.D. Akinwekomi[a], A.A. Adediran[b,*], A.O. Balogun[a], O.G. Olasunkanm[c], T.M.A. Olayanju[d]

[a] Department of Metallurgical and Materials Engineering, Federal University of Technology, Akure PMB 704, Ondo State, Nigeria
[b] Department of Mechanical Engineering, Landmark University, Omu-Aran PMB 1001, Kwara State, Nigeria
[c] Department of Chemistry, Federal University of Technology, Akure PMB 704, Ondo State, Nigeria
[d] Department of Agriculture and Biosystems Engineering, Landmark University, Omu-Aran PMB 1001, Kwara State, Nigeria

ARTICLE INFO

Article history:
Received 25 June 2019
Revised 21 May 2020
Accepted 12 June 2020

Keywords:
Hydrothermal
Hydroxyapatite powder (HAp)
Chicken eggshell
Calcination

ABSTRACT

Nowadays, researchers are exploring the suitability of agricultural wastes as biomaterials to solve biomedical related problems. In this work, we investigated the effect of calcination temperature on the properties of hydrothermally synthesized hydroxyapatite (HAp). Chicken eggshells were obtained from local farm as a waste and were thoroughly washed and boiled in distilled water for 10 min to remove its inherent membranes. The cleaned shells were oven dried for 24 h, and thereafter divided into three parts to carry out a three-stage calcination treatment at 800 °C, 900 °C and 1000 °C, respectively. The calcined samples were separately dispersed in beakers containing 100 ml of distilled water and orthophosphoric acid, and were subjected to vigorous stirring under a mechanical stirrer on a hot plate at 90 °C. Ageing treatment of the samples gave lumped white solids for each samples, and were subsequently pulverised into powders. Scanning electron microscopy (SEM), X-ray diffraction (XRD), and energy dispersive X-ray spectroscopy (EDX), were employed to study the powder morphology, phase components and elemental composition, respectively. It was observed that the HAp synthesized at 1000 °C (HA1000) has a similar stoichiometry ratio (Ca/P = 1.65) with that of natural bone and also has the tendency to agglomerate by creating pores required for body fluid circulation.

Introduction

Tissue engineering deals with the use of biomaterials for tissue and organ restoration [23]. Biomaterials are applied as implants, scaffolds, fixation plates, dental cement and fillings because of their excellent bioactivity and biocompatibility [28]. Both natural and synthetic biomaterials have been studied extensively in the literature [11,27]. However, synthetic biomaterials are of peculiar interest to researchers because of the need to develop materials that can act as replacement for natural ones [16,28].

* Corresponding authors.
E-mail addresses: iooladele@futa.edu.ng (I.O. Oladele), adediran.adeolu@lmu.edu.ng (A.A. Adediran).

https://doi.org/10.1016/j.sciaf.2020.e00452

Hydroxyapatite is an example of synthetic biomaterial with chemical formula $Ca_{10}(PO_4)_6(OH)_2$. It is capable of supporting bone reformation and osseointegration in dental, orthopaedic and maxillofacial applications [3,4,7]. Similar to bone, its biomineral constituents which is majorly calcium and phosphorus, are responsible for facilitating ion exchange with its host [12,13,29]. Studies have shown that hydroxyapatite shows no inflammatory, toxicity and pyrogenetic responses [10]. These aforementioned characteristics of hydroxyapatite are major attractions that encourage its wide usage for solving any bone related problems [1,3].

Nowadays, research is not only geared towards improving hydroxyapatite performance but also cost-cutting its production by making it available in large amount [21]. Several strategies have been developed to synthesize hydroxyapatite into different architectures and morphologies such as powder fillings, dense/porous blocks, or as reinforcement in biocomposites [20]. Notable methods of synthesizing hydroxyapatite powder (HAp) are the sol-gel process, wet-chemical method and hydrothermal technique [22]. Hydrothermal technique is commonly practised due to its ease and low-cost of processing high-quality HAp. The technique involves mixing solid precursor, chemical and water, to form HAp under specific thermal conditions [10,22]. Calcium salts, coral, hollow calcium carbonate ($CaCO_3$) microspheres, mussel shell, snail shell, sea shell, chicken eggshell, and xonotlite [$Ca_6(Si_6O_{17})(OH_2)$] nanowire, are solid precursors that have been studied for HAp synthesis [3,14,24]. Among them, chicken eggshell is of interest in this research because it is readily available at no cost, rich in calcium and can produce HAp that is capable of promoting greater bone reformation [23].

Gergely et al. [7] produced HAp from eggshells by comparing two different mechanochemical techniques (attrition milling and ball milling). In their work, both techniques resulted to HAp formation. However, attrition milling resulted to nanometre sized HAp while ball milling produces micrometre sized HAp with smooth surfaces. Goloshchapov et al. [8] studied the optimal parameters that affect the synthesis of HAp from bird eggshells using precipitation technique. Their result shows that the morphology of HAp is almost preserved at 900ºC resulting to a stoichiometry ratio of Ca/P of 1.67, similar to mineral constituents of bone tissue.

Despite these works on eggshells derived HAp, hydroxyapatite from chicken eggshells of southwest, Nigeria origin has not been reported. The mineralised composition of chicken eggshells depends on factors such as the geographical location, colour, age, body structure and, feeding [17]. It is therefore necessary to examine the suitability of the eggshells for biomedical applications since the stoichiometry ratio from the mineralised composition affects the thermal stability [23].

Due to the growing need of biomaterials to solve biomedical related problems, researchers have started utilizing available agricultural wastes to develop biomaterials in large amount [2]. The emergent agro-wastes that are employed for the production of hydroxyapatite serves as an alternative inorganic source in bones and tooth due to their similar biomineral constituents, and are expected to continue to stimulate the interest of researchers worldwide [18,19].

In Nigeria presently, eggshells are seen as agricultural waste and disposed as non-valuable materials into the environment. As a result of their accumulation, serious threat has been posed to human health and environment due to the microbial actions of the eggshells. To enable sustainable development by adding value to agricultural wastes, these eggshells can be utilized for developing hydroxyapatite for biomedical applications.

In this research, HAp was synthesized from chicken eggshells using hydrothermal method and the effect of varying calcination temperatures on the quality of HAp produced was investigated.

Materials and methods

Materials

Chicken eggshells were obtained from a household poultry farm in Akure, Ondo state, Nigeria. Orthophosphoric acid (H_3PO_4, $\geq$ 99.0%, ACS Reagent) were obtained from Chemistry Department, Federal University of Technology Akure.

Methods

Preparation of eggshells

The eggshells are obtained from eggs of 20-week old black chicken (*Gallus domesticus*), of frizzled feather and naked neck structure with an average body weight of 0.7 $\pm$ 0.24 kg. The collected eggshells were first cleaned, washed and boiled in distilled water for about 10 min to remove its membranes. Then, the cleaned shells were dried for 24 h in an oven at 80 ºC. The dried shells were then weighed and divided into three parts and were placed in a furnace at 800 ºC, 900 ºC and 1000 ºC, respectively. However, for the purpose of convenience, the powder samples were denoted as HA800, HA900, and HA1000 for the three different operating temperatures, respectively.

Calcination of eggshells

The experimental setup for the calcination of eggshells was carried out in accordance with Gergely et al. [7] and Goloshchapov et al. [8], as shown in Fig. 1.

As shown in Table 1, the first stage of the calcination treatment for HA800 sample involves heating the shells up to 350 ºC at a heating rate of 7 ºC/min, and was subsequently followed by soaking at 350 ºC for 4 h. In the second stage, the shells were heated from 350 ºC up to 500 ºC at a heating rate of 5 ºC/min and werealso soaked for 4 h. In the final stage,

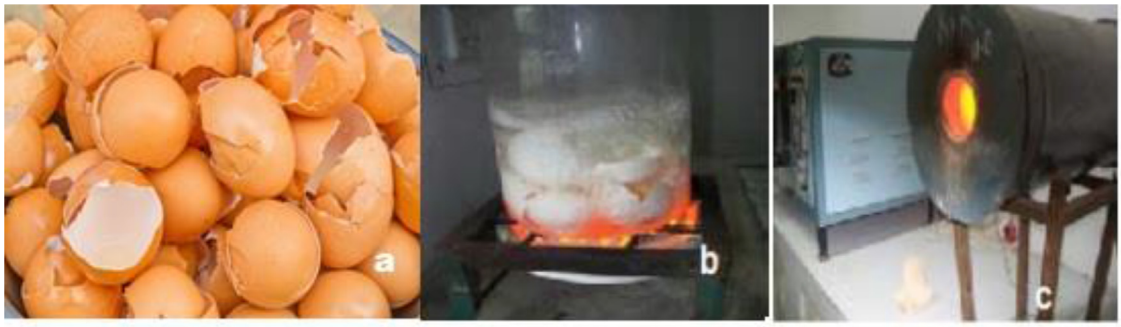

Fig. 1. Experimental setup for eggshells calcination (a) eggshells (b) boiling of eggshells (c) calcination in the furnace.

Table 1
Three stage calcination treatment of HA800 sample.

	Temperature (°C)	Heating rate (°C /min)	Soaking time (h)
Stage1	0-350	7	4
Stage 2	350-500	5	4
Stage 3	500-800	4	3

Table 2
Three stage calcination treatment of HA900 sample.

	Temperature (°C)	Heating rate (°C /min)	Soaking time (h)
Stage 1	0-450	7	3
Stage 2	450-600	5	3
Stage 3	600-900	4	2

Table 3
Three stage calcination treatment of HA1000 sample.

	Temperature (°C)	Heating rate (°C /min)	Soaking time (h)
Stage 1	0-550	7	2
Stage 2	550-700	5	2
Stage 3	700-1000	4	1

the shells were heated from 500 °C to 800 °C at a heating rate of 4 °C/min followed by soaking for 3 h. At 800 °C, the shells have been transformed into calcium oxide (CaO) by evolving carbon(iv)oxide (CO_2) as shown in Eq. (1).

$$CaCO_3 \rightarrow CO_2 + CaO \quad (1)$$

Similarly, HA900 sample was first heated up to 450 °C and soaked at same temperature for 3 h. In the second stage, the shells were heated from 450 °C to 600 °C, and were soaked for 3 h. At the final stage, the shells were heated from 600 °C to 900 °C, followed by soaking for 2 h to transform the shells into CaO by releasing CO_2. The corresponding heating rates for the first, second and third calcination stages are 7 °C/min, 5 °C/min, and 4 °C/min, respectively. The summary of the three-stage calcination treatment of the second part of the dried shells can be seen in Table 2.

Also, HA1000 sample was heated up to 550 °C at a heating rate of 7 °C/min, and was subsequently soaked this same temperature for 2 h. In the second stage, the shells were heated up from 550 °C to 700 °C at a heating rate of 5 °C/min, followed by soaking for 2 h. In the final stage, the shells were heated up from 700 °C to 1000 °C at a heating rate of 4 °C/min, and were soaked for 1 h at 1000 °C. The summary of the three-stage calcination treatment of the third part of the dried shells is presented in Table 3.

Synthesis of hydroxyapatite powder (HAp)

The CaO produced from the calcined eggshell was converted into HAp in an orthophosphoric acid following the procedures reported by Hui et al. [10]. A stoichiometric amount of the calcined samples was separately dispersed in three beakers containing 100 ml of distilled water and were placed on a hot plate for 2 h. Under vigorous stirring at 120 rpm, orthophosphoric acid (20 ml) was added to each of the calcined eggshell mixtures at a controlled temperature of about 90 °C. Initially, a suspension was observed for all the three mixtures (HA800, HA900, and HA1000), however, after about 30 mins of vigorous mixing, a clear mixture was formed for all the three portions. The pH value of the solution at the time was kept below 2 by adding sodium hydroxide solution (2 ml) when needed. Afterwards, the three-sample solutions were subjected to aging treatment for 7 days, before being filtered. The filtered residues were further dried in an oven at 105 °C,

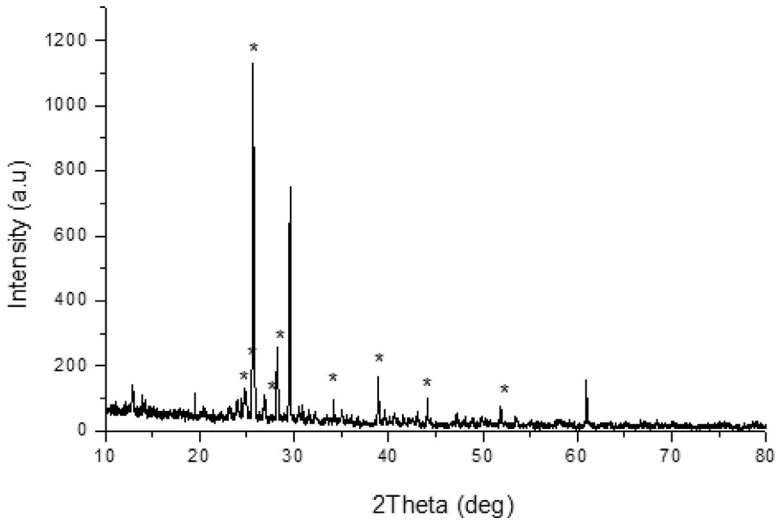

Fig. 2. The X-ray diffraction pattern for HA800 sample.

followed by soaking for 1 h at same temperature. Thereafter, they were heated in a furnace to 800 °C, 900 °C, and 1000 °C, for HA800, HA900 and HA1000 residues, respectively. The heating rate and soaking time were maintained at 15 °C/min and 1 h, respectively. Finally, the lumped hydroxyapatite solids formed were made into powders known to be HAp, and the expected reaction of synthesis is given in Eq. (2).

$$10Ca(OH)_2 + \quad 6H_3PO_4 \rightarrow \quad Ca_{10}(PO_4)_6(OH)_2 + 18H_2O \tag{2}$$

It should be noted that when CaO was dispersed in water, calcium hydroxide might be produced. So, the actual reaction can be seen in Eq. (3).

$$10CaO + 10\ H_2O \ + 6H_3PO_4 \quad \rightarrow Ca_{10}(PO_4)_6(OH)_2 + 18H_2O \tag{3}$$

Characterization of hydroxyapatite (HAp)

Dried white powders were obtained for the three set of samples prepared from HA800, HA900 and HA1000 residues, respectively. XRD, EDX, and SEM studies were conducted to characterize and confirm the dried powder samples produced.

X-ray diffraction (XRD) technique

XRD technique was applied to study the structural characteristics of the dried powder samples. The purpose of the study was to determine the phase composition of the synthesized samples (HA800, HA900, and HA1000). X-ray spectra were obtained from a 9 kW Rigaku SmartLab Diffractometer, operated at 45 kV in the range of $10^o < 2\Theta < 80^o$, using Cu Kα radiation (k = 0.15418 nm), and scanning speed of 14 deg/min.

Scanning electron microscope/energy dispersive X-ray (EDX)

The morphology assessment of the sample was determine using a secondary electron image mode of scanning electron microscope (SEM-Carl Zeiss, Germany) operated at 20 kV. Four runs on different spots on each sample were made to determine the chemical composition and to estimate the Ca/P ratio. The samples preparation procedure includes; sectioning, mounting, grinding, polishing, and gold coating.

Results and discussion

This depicts the results of various HAp characteristics produced from the calcined eggshell samples after reaction with orthophosphoric acid. The results are contained in X-ray spectra as shown in Figs. 1–3 and Tables 4–6. The EDX spectra as shown in Figs. 4–6 as well as Tables 7–9, revealed the stoichiometry ratios of the samples. While the SEM image reveals the microstructure of the samples as shown in Figs. 7–9.

XRD Results

Based on the results presented in both Fig. 1 and Table 4 (a and b), the identified phase in HA800 sample is calcium hydrogen phosphate ($Ca_4H_2(P_3O_{10})_2$). This is in agreement with the data of the Joint Committee on Powder Diffraction Standards and the International Centre of Diffraction Data (JCPDS-ICDD, 1995). As shown in Table 4 (a), the peak list of the detected phase as well as interplanar spacing values and relative intensities for the diffraction lines in the HA800 sample

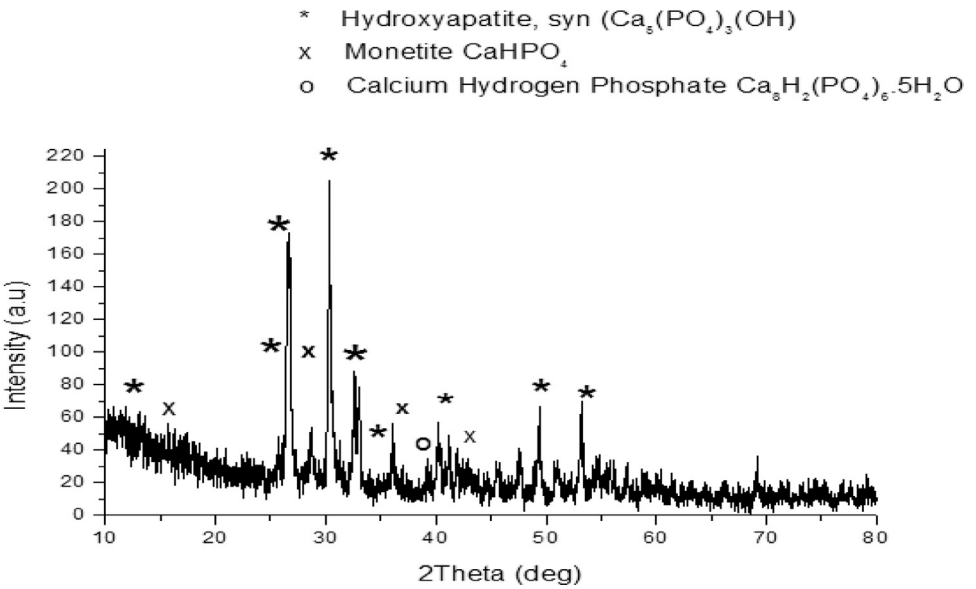

Fig. 3. The X-ray diffraction pattern for HA900 sample.

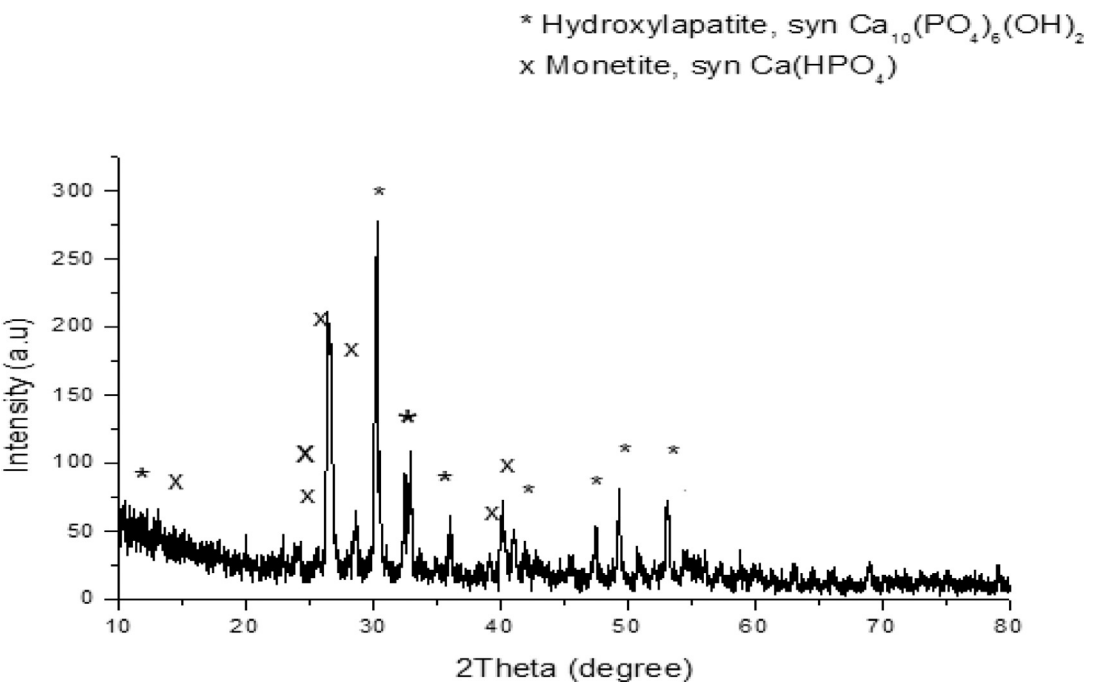

Fig. 4. The X-ray diffraction pattern for HA1000 sample.

confirmed the presence of $Ca_4H_2(P_3O_{10})_2$ all-through. From the XRD data, it was observed that no HAp phase was identified because the temperature is not suitable for it transformation. Hence, the observed phase is similar to the finding of Berezhnaya et al. [5].

Fig. 2 and Table 5 (a and b) shows the XRD results of HA900 sample. The strong peaks identified belong to monetite ($CaHPO_4$), hydroxyapatite ($Ca_{10}(PO_4)_6(OH)_2$), and calcium hydrogen phosphate hydrate ($Ca_8H_2(PO_4)_6{\cdot}5H_2O$) (JCPDS-ICDD, 1995). From Table 5 (b), the major phases are attributed to monetite and hydroxyapatite. From the analysis, $Ca_4H_2(P_3O_{10})_2$ phase was not detected while the presence of $Ca_8H_2(PO_4)_6{\cdot}5H_2O$ phase may be attributed to incomplete transformation of the CaO during calcination process. However, the identified hydroxyapatite phase did not dominate at 900 ^oC as expected.

As shown in Fig. 3 and Table 6 (a and b), the XRD data analysis for the HA1000 sample demonstrated that the powder sample has only monetite and hydroxyapatite (JCPDS-ICDD, 1995). From the analysis, it was observed that the peaks

EDX Results

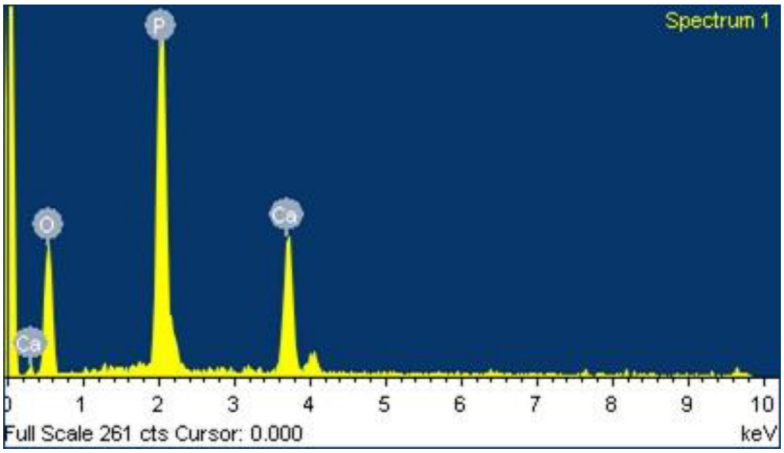

Fig. 5. The Energy-dispersive X-ray spectrum of HA800 sample.

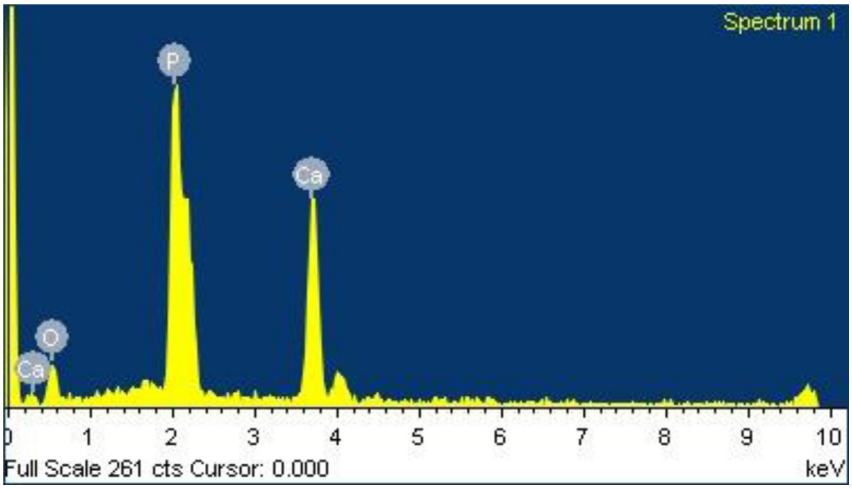

Fig. 6. The Energy-dispersive X-ray spectrum of HA900 sample.

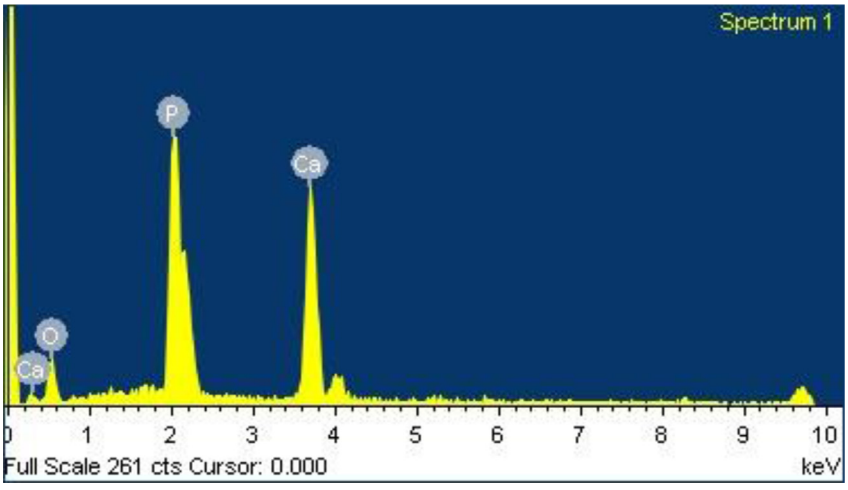

Fig. 7. The Energy-dispersive X-ray spectrum for HA1000 sample.

SEM Images

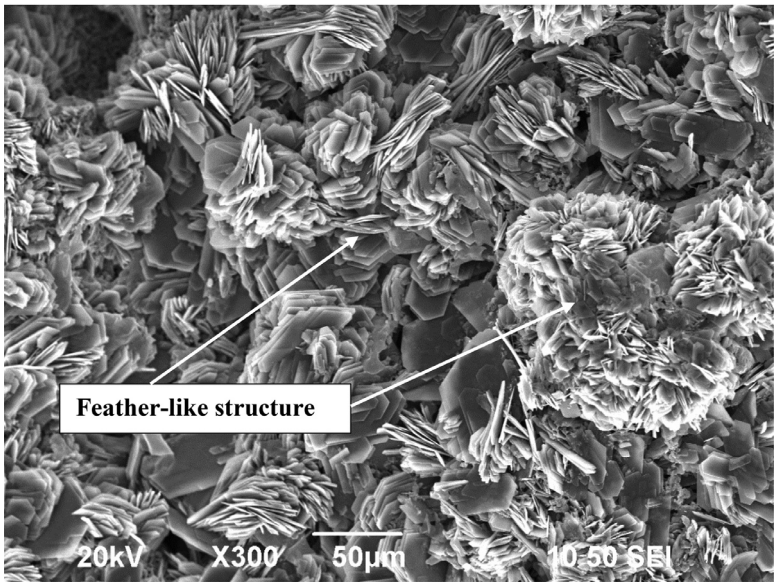

Fig. 8. SEM image of HA800 sample.

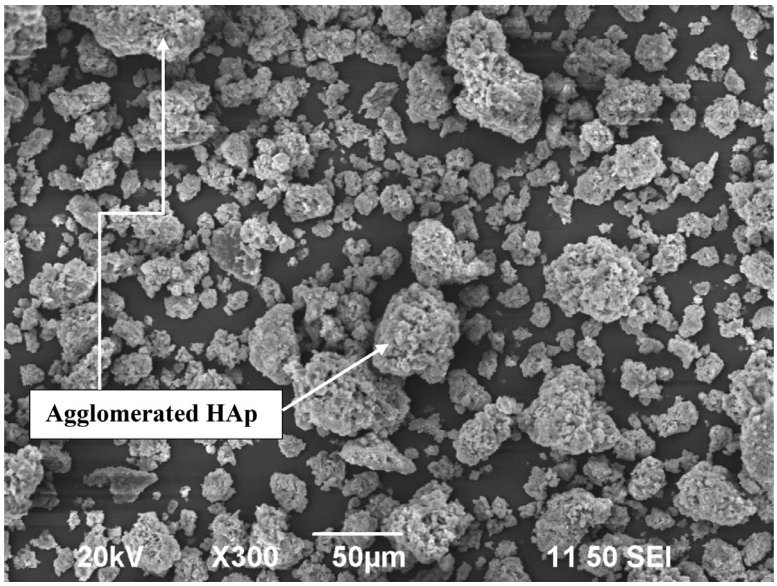

Fig. 9. SEM image of HA900 sample.

of hydroxyapatite dominated the XRD pattern, although, the presence of monetite may still be attributed to incomplete transformation of monetite during calcination. However, the peak list of the detected phases alongside their interplanar spacing values and relative intensities for the diffraction lines in the synthesized HA1000 sample is shown in Table 6(a). It is noteworthy to mention that strong peak of hydroxyapatite phase was clearly identified for HA1000 sample compared with the XRD pattern obtained for HA800 and HA900 samples. Nevertheless, if the calcination temperature is further increased beyond 1000 ^{o}C, we expect that the monetite phase will completely transformed into hydroxyapatite. However, due to the limitation of our homemade furnace which cannot operate beyond 1000 ^{o}C, we decided to focus on the reported temperature range.

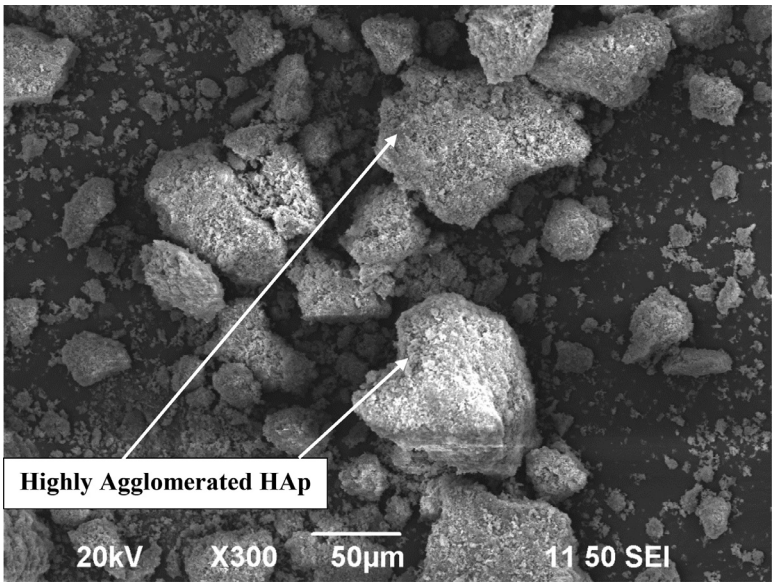

Fig. 10. SEM image of HA1000 sample.

Table 4a
Qualitative analysis of X-ray diffraction results (peak list) for HA800 sample.

No.	2-theta(deg)	d(ang.)	Size(ang.)	Phase name	Chemical formula	DBcard number
1	12.929(8)	6.842(4)	591(79)	Unknown	Unknown	00-000-0000
2	23.96(4)	3.711(6)	424(90)	Unknown	Unknown	00-000-0000
3	24.404(3)	3.6444(5)	1921(635)	Unknown	Unknown	00-000-0000
4	24.83(5)	3.583(7)	226(31)	Calcium Hydrogen Phosphate(0,0,0)	$Ca_4H_2(P_3O_{10})_2$	00-017-0934
5	25.568(3)	3.4811(4)	2409(214)	Unknown	Unknown	00-000-0000
6	25.696(2)	3.4641(3)	1756(109)	Unknown	Unknown	00-000-0000
7	26.84(3)	3.319(3)	550(91)	Unknown	Unknown	00-000-0000
8	28.216(11)	3.1601(12)	456(19)	Calcium Hydrogen Phosphate(0,0,0)	$Ca_4H_2(P_3O_{10})_2$	00-017-0934
9	29.562(4)	3.0193(4)	1599(120)	Unknown	Unknown	00-000-0000
10	30.45(3)	2.933(2)	261(98)	Calcium Hydrogen Phosphate(0,0,0)	$Ca_4H_2(P_3O_{10})_2$	00-017-0934
11	34.170(10)	2.6220(8)	1811(544)	Calcium Hydrogen Phosphate(0,0,0)	$Ca_4H_2(P_3O_{10})_2$	00-017-0934
12	38.891(6)	2.3138(4)	1339(171)	Unknown	Unknown	00-000-0000
13	39.50(4)	2.279(2)	581(161)	Unknown	Unknown	00-000-0000
14	43.028(11)	2.1004(5)	1296(222)	Unknown	Unknown	00-000-0000
15	44.103(9)	2.0517(4)	1442(226)	Calcium Hydrogen Phosphate(0,0,0)	$Ca_4H_2(P_3O_{10})_2$	00-017-0934
16	47.225(10)	1.9231(4)	1205(218)	Unknown	Unknown	00-000-0000
17	53.498(11)	1.7114(3)	665(123)	Unknown	Unknown	00-000-0000
18	58.00(4)	1.5888(10)	153(31)	Calcium Hydrogen Phosphate(0,0,0)	$Ca_4H_2(P_3O_{10})_2$	00-017-0934
19	60.971(6)	1.51835(13)	1953(310)	Unknown	Unknown	00-000-0000

Table 4b
Qualitative analysis of X-ray diffraction results for HA800 sample.

Phase name	Formula	Figure of merit	Phase reg. detail	DB card number
Calcium Hydrogen Phosphate	$Ca_4H_2(P_3O_{10})_2$	1.629	ICDD (PDF2010)	00-017-0934
Phase name	Formula	Space group	Phase reg. detail	DB card number
Calcium Hydrogen Phosphate	$Ca_4H_2(P_3O_{10})_2$	-	ICDD (PDF2010)	00-017-0934

EDX results

The elemental composition and EDX spectrum of HA800 sample is shown in Table 7 and Fig. 4. From the result, it was observed that calcium (Ca), phosphorus (P), and oxygen (O) were identified. We focused on these elements because they are essential mineral constituents for bone growth. “Ca” helps to prevent osteoporosis, “P” helps in bone resorption, while “O” helps to accelerate bone fracture healing [9,25,26]. However, the ratio of calcium to phosphorus (Ca/P) is usually determine for bone reformation and growth during infancy. It is also crucial for preventing adult osteoporosis and poor childhood growth [15]. For this result, the calculated Ca/P is equal to 0.55, which is far below the expected stoichiometry ratio (1.67) of natural bone HAp. Hence, the obtained value shows that HA800 sample is not HAp but another type of calcium phosphate (CP) based biomaterial [3].

Table 5a
Qualitative analysis of X-ray diffraction results (peak list) for HA900 sample.

No.	2-theta(deg)	d(ang.)	Size(ang.)	Phase name	Chemical formula	DB card number
1	26.611(19)	3.347(2)	201(7)	Monetite(2,0,0),Hydroxylapatite, syn(0,1,2),Calcium Hydrogen Phosphate Hydrate(2,-2,-1)	$CaHPO_4$,$Ca_5(PO4)_3$ (OH),Ca8 H2 (P O4)6 •5 H2 O	01-071-1759,01-089-4405,00-026-1056
2	28.68(3)	3.110(3)	581(311)	Monetite(1,1,-2),Calcium Hydrogen Phosphate Hydrate(1,2,-2)	CaHPO4,$Ca8H_2$ (PO4)6 •5 H2 O	01-071-1759,00-026-1056
3	30.335(10)	2.9441(10)	325(16)	Monetite(1,2,0),Hydroxylapatite, syn(0,5,1),Calcium Hydrogen Phosphate Hydrate(1,-2,-2)	Ca HPO_4,$Ca_5(PO_4)_3$(OH),Ca8 H2 (P O4)6 •5 H2 O	01-071-1759,01-089-4405,00-026-1056
4	32.69(6)	2.737(5)	136(10)	Monetite(2,0,1),Hydroxylapatite, syn(-1,4,2),Calcium Hydrogen Phosphate Hydrate(1,4,-2)	$CaHPO_4$,$Ca_5(PO_4)_3$(OH),Ca8 H2 (P O4)6 •5 H2 O	01-071-1759,01-089-4405,00-026-1056
5	40.18(8)	2.242(4)	230(40)	Monetite(0,0,3),Hydroxylapatite, syn(-2,8,1),Calcium Hydrogen Phosphate Hydrate(3,6,1)	CaHPO4,$Ca_5(PO_4)_3$(OH),Ca8 H2 (P O4)6 •5 H2 O	01-071-1759,01-089-4405,00-026-1056
6	41.12(8)	2.194(4)	670(372)	Monetite(0,3,0)	$CaHPO_4$	01-071-1759
7	47.56(7)	1.910(3)	376(94)	Monetite(3,-1,1),Hydroxylapatite, syn(1,7,1),Calcium Hydrogen Phosphate Hydrate(0,5,3)	$CaHPO_4$,$Ca_5(PO_4)_3$(OH),Ca8 H2 (P O4)6 •5 H2 O	01-071-1759,01-089-4405,00-026-1056
8	49.36(6)	1.845(2)	369(77)	Monetite(3,-2,0),Calcium Hydrogen Phosphate Hydrate(1,10,-1)	CaH PO_4,Ca_8 H_2 $(PO_4)_6$ •5 H2 O	01-071-1759,00-026-1056
9	53.20(5)	1.7204(15)	277(28)	Monetite(4,0,-1),Hydroxylapatite, syn(0,0,4)	$CaHPO_4$,$Ca_5(PO4)_3$ (OH)	01-071-1759,01-089-4405
10	54.47(19)	1.683(5)	66(10)	Monetite(2,-2,-3),Hydroxylapatite, syn(-1,1,4)	Ca H PO_4,Ca_5 $(PO4)_3$(O H)	01-071-1759,01-089-4405
11	69.03(14)	1.359(2)	246(64)	Hydroxylapatite, syn(6,0,0)	$Ca5(PO_4)_3$ (OH)	01-089-4405

Table 5b
Qualitative analysis of X-ray diffraction results of HA900 sample.

Phase name	Formula	Figure of merit	Phase reg. detail	DB card number
Monetite	$CaHPO_4$	0.802	ICDD (PDF2010)	01-071-1759
Hydroxylapatite, syn	$Ca_{10}(PO_4)_6(OH)_2$	2.963	ICDD (PDF2010)	01-089-4405
Calcium Hydrogen Phosphate Hydrate	$Ca_8H_2(PO_4)_6$•$5H_2O$	1.823	ICDD (PDF2010)	00-026-1056
Phase name	Formula	Space group	Phase reg. detail	DB card number
Monetite	$CaHPO_4$	2:P-1	ICDD (PDF2010)	01-071-1759
Hydroxylapatite, syn	$Ca_{10}(PO_4)_6(OH)_2$	-	ICDD (PDF2010)	01-089-4405
Calcium Hydrogen Phosphate Hydrate	$Ca_8H_2(PO_4)_6$•$5H_2O$	2:P-1	ICDD (PDF2010)	00-026-1056

Table 8 and Fig. 5 shows the elemental composition and EDX spectrum of HA900 sample. The EDX analysis showed that HA900 sample consists of Ca, P, and O. The Ca/P ratio as calculated from the EDX result is equal to 1.26. From the EDX analysis, it can be deduced that the presence of other phases (such as monetite and calcium hydrogen phosphate hydrate) in the HA900 composition affected the concentration of hydroxyapatite thereby limiting the realization of the expected stoichiometry ratio.

Table 9 and Fig 6 shows the elemental composition and EDX spectrum of HA1000 sample. It can be seen from the results that HA1000 sample consists of Ca, P, and O. Unlike HA800 and HA900, the Ca/P ratio as calculated is equivalent to 1.65, which is closer to the expected stoichiometric ratio of 1.67. From the EDX analysis, it can be deduced that HA1000 sample has the complete hydroxyapatite phase. Although, the presence of monetite phase as revealed by the XRD result, may contribute to why its Ca/P not equal to 1.67.

The SEM image of HA800 sample can be seen in Fig. 7. It can be seen that the SEM image resembles that of a crystallites flake like structure as reported by Chakraborty et al. [6]. Also, it was observed that some of the crystallites agglomerate to form an arbitrary flower-like structure. However, the respective XRD and EDX results as shown in Fig. 1 and Table 4, also give credence to the fact that the SEM image of HA800 is not HAp structure.

The SEM image of HA900 sample as seen Fig. 8 shows an agglomerated HAp sample. The agglomerates are spherical in shape. Most of the individual fine particles were observed to be of similar shape with the commercially available HAp, but showed high tendency to agglomerate by creating pores in between. Hence, the formation of pores may be beneficial as it will permit the circulation of body fluid when the synthesized HA900 sample is applied as biomaterial coating on an implant.

The SEM image of HA1000 sample is shown in Fig. 9. From the image, it is observed that the sample agglomerated to form an irregular shape structure. This indicates that the sample resembles HAp as confirmed from the XRD and EDX results

Table 6a
Qualitative analysis of X-ray diffraction results (peak list) for HA1000 sample.

No.	2-theta(deg)	d(ang.)	Size(ang.)	Phase name	Chemical formula	DB card number
1	26.440(15)	3.3683(19)	200(5)	Monetite, syn(0,0,2),Hydroxylapatite, syn(0,0,2),Hydroxylapatite, syn(0,1,2)	Ca (HPO4),Ca10(PO4)6(OH)2,Ca5 (P O4)3 O H	01-089-5969,01-072-1243,01-076-0694
2	28.50(5)	3.130(5)	322(44)	Monetite, syn(1,1,-2),Hydroxylapatite, syn(1,0,2)	$Ca(HPO_4)Ca_{10}(PO_4)_6(OH)_2$	01-089-5969,01-072-1243
3	30.141(14)	2.9626(14)	253(8)	Monetite, syn(2,-1,0),Hydroxylapatite, syn(0,5,1)	$Ca(HPO_4),Ca_5$(P O4)3 O H	01-089-5969,01-076-0694
4	32.43(4)	2.758(3)	303(54)	Monetite, syn(1,0,2),Hydroxylapatite, syn(1,1,2),Hydroxylapatite, syn(2,-2,2)	$Ca(HPO_4),Ca_{10}$ (P O_4)$_6$ (O H)2,Ca5 (P O4)3 O H	01-089-5969,01-072-1243,01-076-0694
5	32.84(3)	2.725(3)	393(72)	Monetite, syn(2,0,-2),Hydroxylapatite, syn(3,0,0),Hydroxylapatite, syn(2,-1,2)	$Ca(HPO_4),Ca_{10}$ (P O_4)$_6$ (O H)2,Ca5 (P O4)3 O H	01-089-5969,01-072-1243,01-076-0694
6	35.924(12)	2.4978(8)	322(38)	Monetite, syn(0,2,-2),Hydroxylapatite, syn(2,3,1)	$Ca(HPO_4),Ca_5$ (P O_4)$_3$ O H	01-089-5969,01-076-0694
7	40.00(5)	2.252(3)	221(28)	Monetite, syn(1,1,-3),Hydroxylapatite, syn(1,3,0),Hydroxylapatite, syn(0,1,3)	$Ca(HPO_4),Ca_{10}$ (P O_4)$_6$ (O H)2,Ca5 (P O4)3 O H	01-089-5969,01-072-1243,01-076-0694
8	40.98(6)	2.201(3)	332(69)	Monetite, syn(0,1,-3),Hydroxylapatite, syn(1,0,3)	$Ca(HPO_4),Ca_5$ (P O_4)$_3$ O H	01-089-5969,01-076-0694
9	47.435(15)	1.9151(6)	328(53)	Monetite, syn(3,2,-1),Hydroxylapatite, syn(1,7,1)	$Ca(HPO_4),Ca_5$ (P O_4)$_3$ O H	01-089-5969,01-076-0694
10	49.201(16)	1.8504(6)	425(47)	Monetite, syn(3,-2,-1),Hydroxylapatite, syn(3,-3,3)	$Ca(HPO_4),Ca_5$ (P O_4)$_3$ O H	01-089-5969,01-076-0694
11	50.76(11)	1.797(4)	315(147)	Monetite, syn(1,-2,-3),Hydroxylapatite, syn(3,2,1),Hydroxylapatite, syn(3,-1,3)	$Ca(HPO_4),Ca_{10}$ (P O_4)6 (O H)2,Ca5 (P O4)3 O H	01-089-5969,01-072-1243,01-076-0694
12	52.97(2)	1.7273(7)	402(49)	Monetite, syn(3,-2,-2),Hydroxylapatite, syn(1,7,2)	$Ca(HPO_4),Ca_5$ (P O_4)$_3$ O H	01-089-5969,01-076-0694
13	54.43(4)	1.6842(12)	75(10)	Monetite, syn(2,0,3),Hydroxylapatite, syn(0,0,4),Hydroxylapatite, syn(1,-1,4)	$Ca(HPO_4),Ca_{10}$ (P O_4)$_6$ (O H)2,Ca5 (P O4)3 O H	01-089-5969,01-072-1243,01-076-0694

Table 6b
Qualitative analysis of X-ray diffraction results of HA1000 sample.

Phase name	Formula	Figure of merit	Phase reg. detail	DB card number
Monetite, syn	$Ca(HPO_4)$	0.802	ICDD (PDF2010)	01-071-1759
Hydroxylapatite,	$Ca_{10}(PO_4)_6(OH)_2$	2.963	ICDD (PDF2010)	01-089-4405
Hydroxylapatite,	$Ca_{10}(PO_4)_6(OH)_2$	1.823	ICDD (PDF2010)	00-026-1056
Phase name	Formula	Space group	Phase reg. detail	DB card number
Monetite, syn	$Ca(HPO_4)$	1:P1	ICDD (PDF2010)	01-089-5969
Hydroxylapatite,	$Ca_{10}(PO_4)_6(OH)_2$	176:P63/m	ICDD (PDF2010)	01-072-1243
Hydroxylapatite,	$Ca_{10}(PO_4)_6(OH)_2$	14:P1121/b,unique-c, cell-3	ICDD (PDF2010)	01-076-0694

Table 7
Elemental composition of HA800 sample.

Element	Weight%	Atomic%
O	55.57	72.48
P	28.71	19.34
Ca	15.72	8.18
Totals	100.00	

Table 8
Elemental composition of HA900 sample.

Element	Weight%	Atomic%
O	38.15	57.76
P	27.36	21.40
Ca	34.49	20.85
Totals	100.00	

Table 9
Elemental composition of HA1000 sample.

Element	Weight%	Atomic%
O	34.60	60.15
P	24.68	19.01
Ca	40.72	20.83
Totals	100.00	

presented in Fig. 3 and Table 6, respectively. Based on the analysis, the synthesized HAp can be used for making scaffolds of various pore sizes and shapes by mixing with polymers.

Conclusions

The results obtained by synthesizing HAp using hydrothermal processing are summarized below.

1 XRD results showed strong peak of hydroxyapatite phase for sample HA1000 while the EDX results confirmed that the stoichiometry ratio was very close to that of natural bone with a value of 1.65. These imply that, high calcination temperature is suitable for synthesizing high quality hydroxyapatite from chicken eggshell.
2 SEM images revealed different morphologies that correspond to varying synthesized reinforcing materials with HA1000 structure revealing hydroxyapatite.
3 It is expected that more research should be done using other wastes such as crustacean shells, fish bones, corals and red algae, to synthesize hydroxyapatite in large quantity. In particular, higher calcination temperatures above 1000 ^{o}C should be investigated to ascertain the actual temperature that gives the purest hydroxyapatite phase.

Acknowledgement

We appreciate Landmark University Centre for Research, Innovation and Development (LUCRID) for their support towards this work.

References

[1] I. Abdulrahman, H.I. Tijani, B.A. Mohammed, H. Saidu, H. Yusuf, M. Ndejiko Jibrin, S. Mohammed, From garbage to biomaterials: an overview on egg shell based hydroxyapatite, J. Mater. 2014 (2014) 1–6.
[2] N.I. Agbeboh, I.O. Oladele, O.O. Daramola, A.A. Adediran, O.O. Olasukanmi, M.O. Tanimola, Environmentally sustainable processes for the synthesis of hydroxyapatite, Heliyon 6 (4) (2020) e03765.
[3] M. Akram, R. Ahmed, I. Shakir, W.A.W. Ibrahim, R. Hussain, Extracting hydroxyapatite and its precursors from natural resources, J. Mater. Sci. 49 (4) (2014) 1461–1475.
[4] M. Aminzare, A. Eskandari, M.H. Baroonian, A. Berenov, Z.R. Hesabi, M. Taheri, S.K. Sadrnezhaad, Hydroxyapatite nanocomposites: synthesis, sintering and mechanical properties, Ceram. Int. 39 (3) (2013) 2197–2206.
[5] A.Y. Berezhnaya, V.O. Mittova, E.V. Kukueva, I.Y. Mittova, Effect of high- temperature annealing on solid-state reactions in hydroxyapatite/TiO 2 films on titanium substrates, Inorg. Mater. 46 (9) (2010) 971–977.
[6] R. Chakraborty, S. Sengupta, P. Saha, K. Das, S. Das, Synthesis of calcium hydrogen phosphate and hydroxyapatite coating on SS316 substrate through pulsed electrodeposition, Mater. Sci. Eng. 69 (2016) 875–883.
[7] G. Gergely, F. Wéber, I. Lukács, A.L. Tóth, Z.E. Horváth, J. Mihály, C. Balázsi, Preparation and characterization of hydroxyapatite from eggshell, Ceram. Int. 36 (2) (2010) 803–806.
[8] D.L. Goloshchapov, V.M. Kashkarov, N.A. Rumyantseva, P.V. Seredin, A.S. Lenshin, B.L. Agapov, E.P. Domashevskaya, Synthesis of nanocrystalline hydroxyapatite by precipitation using hen's eggshell, Ceram. Int. 39 (4) (2013) 4539–4549.
[9] M. Gowen, Cytokines and Bone Metabolism, CRC Bath, UK, 1992, pp. 71–91.
[10] P. Hui, S.L. Meena, G. Singh, R.D. Agarawal, S. Prakash, Synthesis of hydroxyapatite bio-ceramic powder by hydrothermal method, J. Miner. Mater. Charact. Eng. 9 (8) (2010) 683 JCPDS -ICDD (1995) Card _ 9-432.
[11] R.J. Kane, R.K. Roeder, Effects of hydroxyapatite reinforcement on the architecture and mechanical properties of freeze-dried collagen scaffolds, J. Mech. Behav. Biomed. Mater. 7 (2012) 41–49.
[12] G. Krithiga, T.P. Sastry, Preparation and characterization of a novel bone graft composite containing bone ash and egg shell powder, Bull. Mater. Sci. 34 (1) (2011) 177–181.
[13] M. Li, Q. Liu, Z. Jia, X. Xu, Y. Cheng, Y. Zheng, T. Xi, S. Wei, Graphene oxide/hydroxyapatite composite coatings fabricated by electrophoretic nanotechnology for biological applications, Carbon 67 (2014) 185–197.

[14] K. Lin, X. Liu, J. Chang, Y. Zhu, Facile synthesis of hydroxyapatite nanoparticles, nanowires and hollow nano-structured microspheres using similar structured hard-precursors, Nanoscale 3 (8) (2011) 3052–3055.
[15] E. Loughrill, D. Wray, T. Christides, N. Zand, Calcium to phosphorus ratio, essential elements and vitamin D content of infant foods in the UK: possible implications for bone health, Matern. Child Nutr. 13 (3) (2017) e12368.
[16] M.F. Maitz, Applications of synthetic polymers in clinical medicine, Biosurf. Biotribology 1 (3) (2015) 161–176.
[17] L.O. Ojedapo, O. Akinokun, T.A. Adedeji, T.B. Olayeni, S.A. Ameen, A.O. Ige, S.R. Amao, Evaluation of growth traits and short-term laying performance of three different strains of chicken in the derived savannah zone of Nigeria, Int. J. Poul. Sci. 7 (1) (2008) 92–96.
[18] I.O. Oladele, O.G. Agbabiaka, O.G. Olasunkanmi, A.O. Balogun, M.O. Popoola, Non-synthetic sources for the development of hydroxyapatite, J. Appl. Biotechnol. Bioeng. 5 (2) (2018) 92–99.
[19] I.O. Oladele, O.S. Akinola, O.G. Agbabiaka, J.A. Omotoyinbo, Mathematical model for the prediction of impact energy of organic material based hydroxyapatite (HAp) reinforced epoxy composites, Fibers Polym. 19 (2) (2018) 452–459.
[20] I.O. Oladele, O.G. Agbabiaka, A.A. Adediran, A.D. Akinwekomi, A.O. Balogun, Structural performance of poultry eggshell derived hydroxyapatite based high density polyethylene bio-composites, Heliyon 5 (10) (2019) e02552.
[21] I.R. Oliveira, T.L. Andrade, K.C.M.L. Araujo, A.P. Luz, V.C. Pandolfelli, Hydroxyapatite synthesis and the benefits of its blend with calcium aluminate cement, Ceram. Int. 42 (2) (2016) 2542–2549.
[22] M. Othmani, A. Aissa, A. Grelard, R.K. Das, R. Oda, M. Debbabi, Synthesis and characterization of hydroxyapatite-based nanocomposites by the functionalization of hydroxyapatite nanoparticles with phosphonic acids, Colloids Surf. A 508 (2016) 336–344.
[23] S.K. Padmanabhan, L. Salvatore, F. Gervaso, M. Catalano, A. Taurino, A. Sannino, A. Licciulli, Synthesis and characterization of collagen scaffolds reinforced by eggshell derived hydroxyapatite for tissue engineering, J. Nanosci. Nanotechnol. 15 (1) (2015) 504–509.
[24] A. Shavandi, A.E.D.A. Bekhit, A. Ali, Z. Sun, Synthesis of nano-hydroxyapatite (nHA) from waste mussel shells using a rapid microwave method, Mater. Chem. Phys. 149 (2015) 607–616.
[25] B.J. Shea, J.D. Adachi, A. Cranney, L. Griffith, G. Guyatt, C. Hamel, G. Wells, Calcium supplementation on bone loss in postmenopausal women, Cochrane Database Syst. Rev. (1) (2004) 1–20.
[26] C.J. Vorland, E.R. Stremke, R.N. Moorthi, K.M.H. Gallant, Effects of excessive dietary phosphorus intake on bone health, Curr. Osteoporos. Rep. 15 (5) (2017) 473–482.
[27] M.T. Wolf, C.L. Dearth, S.B. Sonnenberg, E.G. Loboa, S.F. Badylak, Naturally derived and synthetic scaffolds for skeletal muscle reconstruction, Adv. Drug. Deliv. Rev. 84 (2015) 208–221.
[28] S.M. Zakaria, S.H. Sharif-Zein, M.R. Othman, F. Yang, J.A. Jansen, Nanophase hydroxyapatite as a biomaterial in advanced hard tissue engineering: a review, Tissue Eng. Part B 19 (5) (2013) 431–441.
[29] L. Zhang, W. Liu, C. Yue, T. Zhang, P. Li, Z. Xing, Y. Chen, A tough graphene nanosheet/hydroxyapatite composite with improved in vitro biocompatibility, Carbon 61 (2013) 105–115.